Progress In Electromagnetics Research Letters, Vol. 81, 121–126, 2019

High Impedance Transforming Dual-Band Balun with Isolation and Output Ports Matching

Rahul Gupta[1, *], Mohammad H. Maktoomi[1], Vikas V. Singh[1], and Mohammad S. Hashmi[1, 2]

Abstract—A dual-band balun with inherent impedance transformation is presented in this paper. The inherent impedance transformation ratio from a range of 0.4 to 4.0 makes the balun ideal for the on-chip fabrication. The proposed dual-band balun exhibits excellent input port matching, equal output signal with phase difference of 180°, and extremely good isolation and matching at the output ports. A table is provided with the design parameters at the extreme impedance transformation ratios. The design concept of the proposed balun has been validated through a prototype fabricated on a Rogers RO5880 substrate. The measurement results are in good agreement with the EM simulation measurements.

1. INTRODUCTION

Balun finds usefulness in wide ranging applications such as antenna arrays, balanced mixers, and amplifiers [1]. The key metrics for a balun are balanced phase and magnitude at the differential outputs and the impedance matching at all the ports. The emergence of wireless communication devices has also necessitated miniaturized baluns, with good isolation between the output ports, able to provide good performance at multiple frequencies [2–5]. Furthermore, an added feature of baluns is their impedance transformation ability as this could be extremely useful in applications such as power amplifiers and rectifying antennas in energy harvesting [1, 6, 7]. An added degree of flexibility can be obtained in the DGS structure in [6] whereas the additional burden on impedance transformer could be avoided in [7] with an inherent impedance transforming component in RF front end system. Another importance of high impedance transformation ratio (ITR) with the baluns can be easily identified in on-chip antennas and antenna feedings [6, 8–12]. However, the reported multi-band balun design techniques are not able to provide good impedance transformation and therefore have limited usefulness in niche and emerging energy harvesting applications. A step by step procedure is given in [8] enforcing the need of fixed feedline of 50 Ω impedance which can be relaxed using the proposed balun in the case of a differential feeding. The reports in [9–12] illustrate the need of an additional impedance transformer which can be avoided using the proposed DBB. There are reports on the impedance transforming baluns [13–15]; however, impedance transformations with dual-band operations are rare.

In this paper, a dual-band balun (DBB) with matching at all the ports and very good isolation between the output ports is reported. A simplified analysis and design scheme augmented by the even-odd mode technique facilitates the presented concept. The capability of the presented design technique is demonstrated through a very good agreement between the EM simulated and experimental results. Furthermore, it has been shown that the proposed design can provide high ITR between the input and output port impedances, i.e., high transformation between Z_L and Z_S.

Received 16 November 2018, Accepted 23 January 2019, Scheduled 4 February 2019

* Corresponding author: Rahul Gupta (rahul@iiitd.ac.in).

[1] Department of Electronics and Communication Engineering, IIIT Delhi, New Delhi 110020, India. [2] Department of Electrical and Computer Engineering, Nazarbayev University, Astana 010000, Kazakhstan.

2. PROPOSED CIRCUIT AND ANALYSIS

The architecture of the proposed DBB, in Fig. 1, is symmetric to the X-axis and consists of port 1 as input port and ports 2 and 3 as output ports. It incorporates stubs to short the two coupled-line sections perpendicular to the X-axis. An isolation resistor R (Ω) is incorporated to provide the isolation between the output ports. The characteristic impedances denoted by Z and the electrical lengths denoted by θ of all the transmission lines (TL) are in Ohms (Ω) and degrees ($^\circ$), respectively. Apparently, even-odd mode analysis can be carried out to simplify the design process. Here, the even mode (e) and odd-mode (o) parameters must satisfy conditions in Eq. (1) for a balun architecture to ensure matching at all the ports, balanced outputs, and good isolation between output ports.

$$S_{21e} = 0; \quad S_{22e} = 0; \quad S_{11o} = 1/3 \tag{1}$$

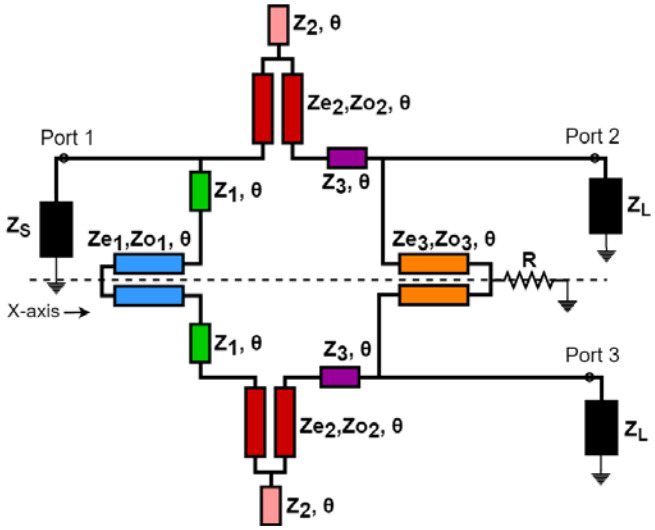

Figure 1. The proposed dual-band balun architecture.

3. DESIGN ANALYSIS AND PROCEDURE

All the TL are considered ideal in the analysis stage. In the even mode circuit, Fig. 2, no signal flows in from port 1, and this is ensured by achieving $Z_{INe} = 0$. For this, the node M should be short circuited, and this results in Eq. (2). Here, Z_1 is an independent variable and should be chosen in the range of [20–150 Ω] so that all the design parameters are realizable. Here, the electrical length follows $\theta = \pi/1 + r$ and r being the desired frequency ratio.

$$Z_{e1} = Z_1 \tan^2\theta \tag{2}$$

In the odd mode circuit, Fig. 2, the term Y_{INoB} is of the form $R_{Bo} \pm jX_{Bo}$. It is the combined admittance of Z_S, Section A, and Section B looking towards Section B. It is matched by an L-type impedance transformer, the Section C having Z_{e2}, Z_{o2}, Z_2 as independent variables, which is considered good for high ITR [16]. Subsequently, the dependent parameters are computed from Eqs. (3) and (4).

$$Z_3 = \frac{-1 \pm \sqrt{1 - \left({R_{Bo}}^2 + {X_{Bo}}^2 - Z_o R_{Bo} - Z_o R_{Bo} \tan^2\theta\right)}}{\tan\theta} \tag{3}$$

$$Z_{o3} = \frac{{Z_3}^3 \tan^2\theta + 2{Z_3}^2 \tan\theta + Z_3 {R_{Bo}}^2 + Z_3 {X_{Bo}}^2}{Z_3 X_{Bo} \left(\tan^2\theta - 1\right) \tan\theta + \left({R_{Bo}}^2 + {X_{Bo}}^2 - {Z_3}^2\right) \tan^2\theta} \tag{4}$$

Furthermore, for the matching at the output ports and for isolation between the output ports, the sufficient condition in even mode is $S_{22e} = 0$. Here, node M is shorted, and hence the input impedance

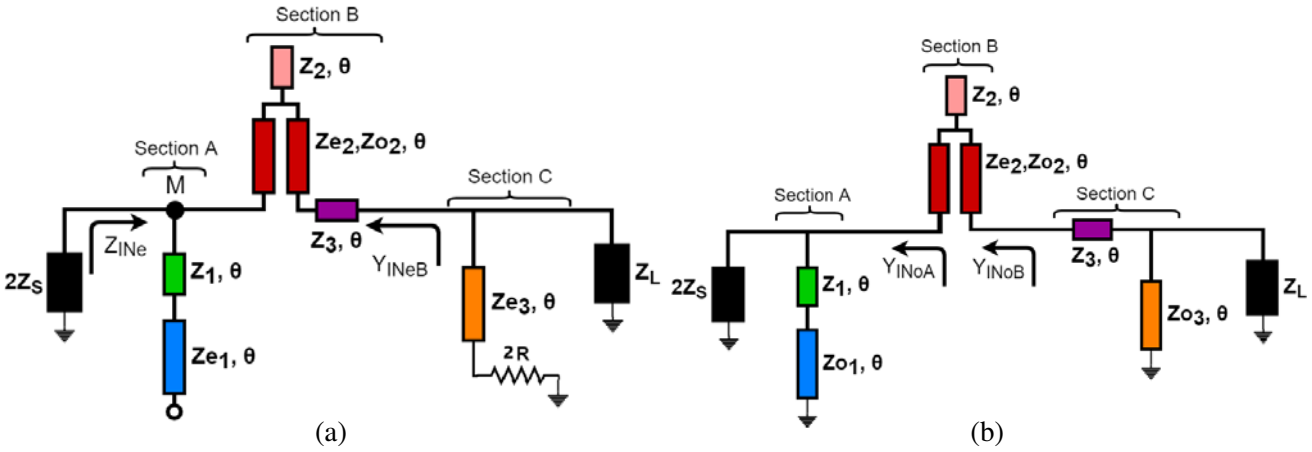

Figure 2. Even mode (a) and odd mode (b) equivalent circuit.

Y_{INeB}, in the form $0 \pm jX_{Be}$, in parallel with the section C can be matched using the calculated values of Z_{e3} and R as outlined in Eqs. (5) and (6).

$$Z_{e3}{}^2\left(2Z_L{}^2R + 2X_{Be}{}^2R \mp Z_LX_{Be}{}^2\right) + Z_{e3}\left(2Z_L{}^2R + 2RX_{Be}{}^2 \mp \frac{4R^2Z_LX_{Be}}{Z_{e3}}\right)\tan^2\theta = 0 \quad (5)$$

$$Z_{e3}{}^2\left(Z_L{}^2X_{Be} - Z_L{}^2\tan\theta - X_{Be}{}^2\tan\theta\right) + 4R^2\tan\theta\left(Z_L{}^2X_{Be}\tan\theta - Z_L{}^2 - X_{Be}{}^2\right) = 0 \quad (6)$$

4. FABRICATION AND MEASUREMENT

A prototype working at 1/2 GHz is designed on Rogers RO5880 to validate the presented concept. The source (load) impedance is taken as 50 Ω so that they gel with the impedances of the SMA connectors and to discard the need of additional impedance transformer. The design equations are used to determine the design parameters as (units: Ω) $Z_1 = 30$, $Z_{e1} = 90$, $Z_{o1} = 62.1$, $Z_2 = 118.7$, $Z_{e2} = 58.4$, $Z_{o2} = 41.3$, $Z_3 = 74.5$, $Z_{e3} = 57.5$, $Z_{o3} = 52.9$, and $R = 55.4$. Electrical lengths of all the TL are chosen as 60° for the dual-band operation. The EM simulations are carried out in CAD tool, and the design parameters are optimized for the TL discontinuities and substrate losses. The prototype with the optimized parameters

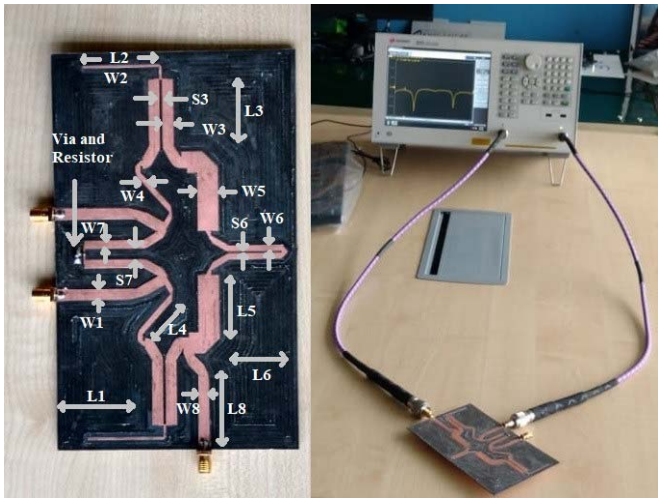

Figure 3. The fabricated prototype (a) and measurement setup (b).

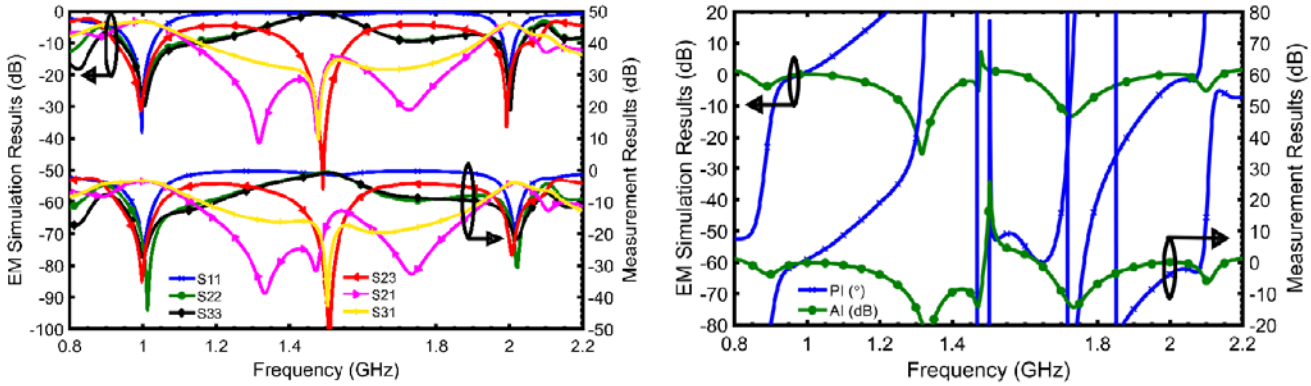

Figure 4. S-parameters (a), Amplitude Imbalance (AI) and Phase Imbalance (PI) (b) results of the fabricated prototype.

is shown in Fig. 3 with dimensions as (units: mil) $W_1 = 185$, $L_1 = 1227.4$, $W_2 = 45$, $L_2 = 1276.7$, $W_3 = 190$, $S_3 = 40$, $L_3 = 1076.7$, $W_4 = 91.7$, $L_4 = 739.8$, $W_5 = 350$, $L_5 = 960.1$, $W_6 = 95$, $L_6 = 861.2$, $S_6 = 30$, $W_7 = 140$, $S_7 = 185$, $L_7 = 992.1$, $W_8 = 185$, $L_8 = 1208.1$, and $R = 56.2\,\Omega$. The EM simulation results and measurement results are shown in Fig. 4. The EM results confirm equal power distribution and matching at all the ports along with good isolation for a broad range of frequencies at both the chosen bands. The measured responses for the amplitude (phase) imbalance are 0.1 dB (0.8°) at 1.0 GHz and 0.0 dB (−3.6°) at 2.0 GHz, and the matching responses S_{11}, S_{22}, and S_{33} are −23.4 dB (−18.9 dB), −44 dB (−30.6 dB), −27.8 dB (−22.2 dB), respectively at 1.0 GHz (2.0 GHz). The insertion losses S_{21} and S_{31} are better than −3.4 dB (−4.5 dB) at the operating frequency of 1.0 GHz (2.0 GHz). Extremely good isolation of −35.1 dB (−26.8 dB) at 1.0 GHz (2.0 GHz) is also achieved in the proposed DBB.

Moreover, the 10 dB bandwidth for S_{11} (S_{22}, S_{33} and S_{23}) at 1 GHz is 0.969–1.034 GHz (0.95–1.17 GHz, 0.94–1.20 GHz, and 0.927–1.06 GHz) and at 2 GHz is 1.99–2.04 GHz (1.97–2.06 GHz, 1.94–2.08 GHz, and 1.96–2.06 GHz). The amplitude (phase) imbalance of 1 dB (5°) is also achieved for a BW of 0.95–1.1 GHz (0.929–1.06 GHz) at 1 GHz and of 1.92–2.06 (1.98–2.10 GHz) at 2 GHz. These results apparently match very well with the simulation results and thereby validate the design concept.

5. APPLICATION FOR IMPEDANCE TRANSFORMATION

An added feature of the proposed DBB is its potential to operate at wide range of distinct load and source impedances. For example, the design parameters (units: Ω) of the DBB for two design cases of maximum achievable ITR of 0.4 and 4.0 are given in Table 1. Electrical lengths of the TL are again 60° for its dual-band operation at 1/2 GHz. The simulation results, in Fig. 5, for these cases also demonstrate the effectiveness of the proposed technique. The two figures on the top demonstrate the performance of

Table 1. Design parameters for two cases of very high ITR.

ITR $(Z_L/Z_S) = 20/50$				**ITR** $(Z_L/Z_S) = 200/50$			
Parameter	Value	Parameter	Value	Parameter	Value	Parameter	Value
Z_1	40	Z_2	105	Z_1	29.1	Z_2	149.8
Z_{e1}	120	Z_3	35.7	Z_{e1}	87.3	Z_3	89
Z_{o1}	87.6	Z_{e3}	22.2	Z_{o1}	79	Z_{e3}	117
Z_{e2}	75.2	Z_{o3}	20.2	Z_{e2}	47.5	Z_{e3}	112
Z_{o2}	57.6	R	14.5	Z_{o2}	29	R	377.7

the balun for ITR 0.4. One figure, on the left, demonstrates the return loss at all the three ports, i.e., S_{11}, S_{22}, and S_{33}, isolation between the two output ports, i.e., S_{23}, and the insertion losses at the two output ports, i.e., S_{21}, and S_{31}. Another figure, on the right, demonstrates the amplitude difference between the two output ports, i.e., amplitude imbalance (AI) and the deviation in the phase from the required phase difference of 180° between the two output ports, i.e., phase imbalance (PI). Similarly, the bottom two figures of Fig. 5 demonstrate all the performance parameters for ITR 4.0. These results therefore confirm the capability of the design to provide inherent impedance transformation integrated with the operation of a balun for a wide range of impedance transformation ratios. However, the design follows a trade-off between the bandwidth and the impedance transformation ratio [17].

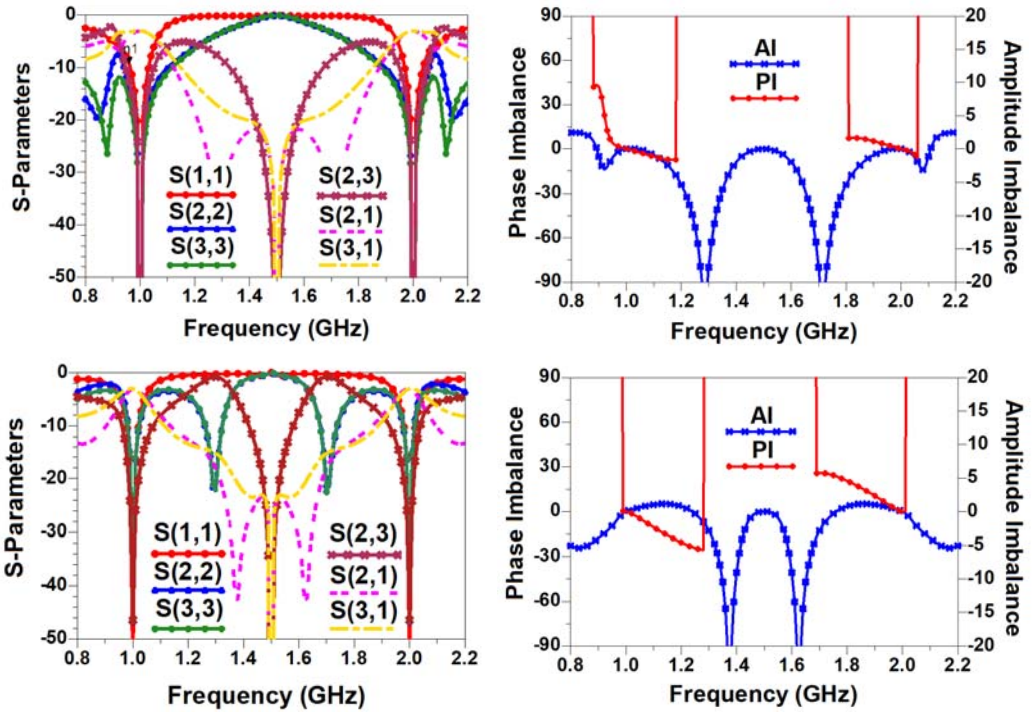

Figure 5. Simulation results of the design for ITR as 0.4 : 1 (top two) and ITR as 4.0 : 1 (bottom two).

6. CONCLUSION

An interesting DBB architecture capable of enhancing all the figures of merit has been proposed. One of the key features of the proposed DBB is its potential to operate at wide range of distinct load and source impedances. It has been shown that the ITR from 0.4 to 4.0 are achievable using the proposed design. A direct application of the proposed DBB is the RF energy harvesting system and on-chip antennas where wide range of ITR could be extremely beneficial.

ACKNOWLEDGMENT

This research was partially funded by ORAU Project at Nazarbayev University, Astana, Kazakhstan. The authors also acknowledge the financial support from MEITY, Govt of India for funding this research through its Visvesvaraya YFRF Scheme.

REFERENCES

1. Oh, H., W. Lee, and H. Lee, "A better balun? done the design of a 4 : 1 wideband balun using a parallel-connected transmission-line balun," *Microw. Magaz.*, Vol. 18, No. 1, 85–90, 2017.
2. Zhang, W., Y. Wu, W. Wang, and X. Shen, "Planar compact dual-band coupled-line balun with high isolation," *China Commun.*, Vol. 14, 40–48, 2017.
3. Yao, L., Y. Wu, M. Li, and Y. Liu, "Three-dimensional high-isolated dual-band balun using double-sided parallel-strip line with inserted conductor plane," *Electron. Lett.*, Vol. 53, 1211–1213, 2017.
4. Ahn, H.-R. and T. Itoh, "New isolation circuits of compact impedance-transforming 3-dB baluns for theoretically perfect isolation and matching," *Trans. Microw. Theory Techn.*, Vol. 58, No. 12, 3892–3902, 2010.
5. Wu, Y., L. Yao, W. Zhang, W. Wang, and Y. Liu, "A planar dual-band coupled-line balun with impedance transformation and high isolation," *IEEE Access*, Vol. 4, 9689–9701, 2016.
6. Aboualalaa, M., A.-B. Abdel-Rahman, A. Allam, H. Elsadek, and R.-K. Pokharel, "Design of a dual-band microstrip antenna with enhanced gain for energy harvesting applications," *Antennas Wirel. Propag. Lett.*, Vol. 16, 1622–1626, 2017.
7. Kanaya, H., T. Nakamura, K. Kawakami, and K. Yoshida, "Design of coplanar waveguide matching circuit for RF-CMOS front-end," *Electron. Commun. Jpn II*, Vol. 88, No. 7, 1017–1023, 2005.
8. Li, X., L. Yang, S.-X. Gong, and Y.-J. Yang, "Dual-band and wideband design of a printed dipole antenna integrated with dual-band balun," *Progress In Electromagnetics Research Letters*, Vol. 6, 165–174, 2009.
9. Xian, J. Z., X. Q. Lin, L. Y. Nie, J. W. Yu, and Y. Fan, "Wideband dual-polarization patch antenna array with parallel strip line balun feeding," *IEEE Antennas Wireless Propag. Lett.*, Vol. 15, 1499–1501, 2016.
10. Yu, J., Y. Sun, H. Zhu, F. Li, and Y. Fang, "Stacked-patch dual-band and dual-polarized antenna with broadband baluns for WiMAX and WLAN applications," *Progress In Electromagnetics Research M*, Vol. 68, 41–52, 2018.
11. Zhang, Z., M. F. Iskander, J. C. Langer, and J. Mathews, "Dual-band WLAN dipole antenna using an internal matching circuit," *IEEE Trans. Antennas Propagat.*, Vol. 53, No. 5, 1813–1818, 2005.
12. Gao, J. P., X. X. Yang, J. S. Zhang, and J. X. Xiao, "A printed volcano smoke antenna for UWB and WLAN communications," *Progress In Electromagnetics Research Letters*, Vol. 4, 55–61, 2008.
13. Ahn, H., and T. Itoh, "Isolation circuit of impedance-transforming 3-dB compact baluns for near perfect output matching and isolation," *IEEE MTT-S International Microwave Symposium*, Anaheim, CA, 113–116, 2010.
14. Zhang, W., Y. Liu, Y. Wu, W. Wang, M. Su, and J. Gao, "A Complex Impedance-Transforming Coupled-Line Balun," *Progress In Electromagnetics Research Letters*, Vol. 48, 123–128, 2014.
15. Gupta, R., and M. S. Hashmi, "High impedance transforming simplified Balun architecture in microstrip technology," *Microw. Optical Technol. Lett.*, Vol. 60, No. 12, 3019–3023, 2018.
16. Nikravan, M.-A., and Z. Atlasbaf, "T-section dual-band impedance transformer for frequency-dependent complex impedance loads," *Electron. Lett.*, Vol. 47, No. 9, 551–553, 2011.
17. Monzon, C., "Analytical derivation of a two-section impedance transformer for a frequency and its first harmonic," *IEEE Microw. Wirel. Compon. Lett.*, Vol. 12, No. 10, 381–382, Oct. 2002.